3-D Coordination Network Structures Constructed from $[W_6S_8(CN)_6]^{6-}$ Anions

Song Jin and Francis J. DiSalvo*

Baker Laboratory, Department of Chemistry and Chemical Biology, Cornell University, Ithaca, New York 14853

Received January 28, 2002. Revised Manuscript Received June 3, 2002

Octahedral molybdenum and tungsten clusters face-capped by chalcogens M_6Q_8 (M = Mo, W; Q = S, Se, Te) have drawn extensive attention because of the well-known molybdenum-based Chevrel phases. Water-soluble cyanide complexes of these clusters can be prepared by cluster excision from the solid-state compound Mo_6Se_8 or by ligand exchange from W_6S_8-(4-*tert*-butylpyridine)$_6$. The $[W_6S_8(CN)_6]^{6-}$ cluster anion can, in turn, be used as a building block to construct 3-D extended coordination networks with transition metal cations M^{2+} (M = Mn, Fe, Co, Zn) as linking units. The novel 3-D structures were determined by X-ray crystallography to be two-fold interpenetrating distorted cubic networks of $[M^{(II)}(H_2O)_4]_3[W_6S_8(CN)_6]\cdot xH_2O$ ($x \approx 23$; M = Mn, Fe, Co) or a rutile-like network of $K_2[Zn(H_2O)_2]_2[W_6S_8(CN)_6]\cdot 26H_2O$, both bridged through W−CN−M−NC−W linkages. The properties of the new network structures are investigated and factors relevant to the construction of network structures containing W_6S_8 clusters are discussed.

Introduction

Octahedral chalcogenide clusters of group VI metals (M_6Q_8, M = Cr, Mo, W; Q = S, Se, Te)[1] have been intensively studied by this[2−6] and many other[7−12] groups partially because the molybdenum clusters of this type (Mo_6Q_8, Q = S, Se, Te) are the building blocks of the solid-state Chevrel phases.[13] Inspired by the remarkable physical properties and applications of Chevrel phases, such as superconductivity,[14] fast ionic conductivity,[15,16] thermoelectric properties,[17,18] and catalytic activity,[19−21] we are interested in constructing novel extended structures with these M_6Q_8 cluster building blocks in anticipation of interesting physical properties.

After the solid-state synthesis of $[Mo_6Se_8(CN)_6]^{7-/6-}$ clusters was reported by Fedorov et al.[22] and Hughbanks et al., [23] we were able to prepare the $[W_6S_8(CN)_6]^{6-}$ cluster anion from neutral molecular $W_6S_8L_6$ clusters in solution and demonstrate its general stability in *deoxygenated* water.[24] Taking advantage of the bidentate nature of the cyanide ligand[25] and learning from the diverse chemistry of cyanide networks,[26−28] we can readily imagine some possible network construction schemes using the $[W_6S_8(CN)_6]^{6-}$ cluster anion as the building block:

(I) $[W_6S_8(CN)_6]^{6-} + M^{n+} \rightarrow [W_6S_8(CN)_6M_m]^{nm-6}$
bridge "W−C≡N−M−N≡C−W"

(II) $[W_6S_8(CN)_6]^{6-} + \{M_6X_8\}^{4+} \rightarrow [W_6S_8(CN)_6M_6X_8]^{2-}$
bridge "W−C≡N−M" (M = Mo, W; X = Cl, Br, I)

(III) $[W_6S_8(CN)_6]^{6-} + W_6S_8L_6 \rightarrow 2[W_6S_8(CN)_3]^{3-} + 6L$
bridge "W−C≡N−W"

The incarnation of type I network building in octahedral $[Re_6Q_8(CN)_6]^{4-/3-}$ (Q = Se, Te) clusters, termed "expanded Prussian blue analogues", has been demon-

* To whom correspondence to be addressed. E-mail: fjd3@cornell.edu. Telephone number: 607-255-7238. Fax: 607-255-4137.

(1) Saito, T. *Adv. Inorg. Chem.* **1997**, *44*, 45.
(2) Ehrlich, G. M.; Warren, C. J.; Vennos, D. A.; Ho, D. M.; Haushalter, R. C.; DiSalvo, F. J. *Inorg. Chem.* **1995**, *34*, 4454.
(3) Venkataraman, D.; Rayburn, L. L.; Hill, L. I.; Jin, S.; Malik, A.-S.; Turneau, K. J.; DiSalvo, F. J. *Inorg. Chem.* **1999**, *38*, 828.
(4) Jin, S.; Venkataraman, D.; DiSalvo, F. J. *Inorg. Chem.* **2000**, *39*, 2747.
(5) Hill, L. I.; Jin, S.; Zhou, R.; Venkataraman, D.; DiSalvo, F. J. *Inorg. Chem.* **2001**, *40*, 2660.
(6) Jin, S.; Zhou, R.; Scheuer, E. M.; Adamchuk, J.; Rayburn, L. L.; DiSalvo, F. J. *Inorg. Chem.* **2001**, *40*, 2666.
(7) Saito, T.; Yamamoto, N.; Yamagata, T.; Imoto, H. *J. Am. Chem. Soc.* **1988**, *110*, 1646.
(8) Saito, T.; Yoshikawa, A.; Yamagata, T. *Inorg. Chem.* **1989**, *28*, 3588.
(9) Hilsenbeck, S. J.; Young, V. G., Jr.; McCarley, R. E. *Inorg. Chem.* **1994**, *33*, 1822.
(10) Xie, X. B.; McCarley, R. E. *Inorg. Chem.* **1995**, *34*, 6124.
(11) Zhang, X.; McCarley, R. E. *Inorg. Chem.* **1995**, *34*, 2678.
(12) Xie, X. B.; McCarley, R. E. *Inorg. Chem.* **1997**, *36*, 4665.
(13) Chevrel, R.; Sergent, M.; Prigent, J. *J. Solid State Chem.* **1971**, *3*, 515.
(14) Chevrel, R.; Sergent, M. In *Topics in Current Physics*; Fischer, O., Maple, M. B., Eds.; Springer-Verlag: Heidelberg, Germany, 1982; Vol. 32, p 25.
(15) Mulhern, P. J.; Haering, R. R. *Can. J. Phys.* **1984**, *62*, 527.
(16) Aurbach, D.; Lu, Z.; Schechter, A.; Gofer, Y.; Gizbar, H.; Turgeman, R.; Cohen, Y.; Moshkovich, M.; Levi, E. *Nature* **2000**, *407*, 724.
(17) Roche, C.; Pecheur, P.; Toussaint, G.; Jenny, A.; Scherrer, H.; Scherrer, S. *J. Phys.: Condens. Matter* **1998**, *10*, L333.
(18) Caillat, T.; Fleurial, J. P.; Snyder, G. J. *Solid State Sci.* **1999**, *1*, 535.
(19) McCarty, K. F.; Anderegg, J. W.; Schrader, G. L. *J. Catal.* **1985**, *93*, 375.
(20) Kaiser, A. B. *Phys. Rev. B: Condens. Matter* **1987**, *35*, 4677.
(21) Hilsenbeck, S. J.; McCarley, R. E.; Thompson, R. K.; Flanagan, L. C.; Schrader, G. L. *J. Mol. Catal. A-Chem.* **1997**, *122*, 13.
(22) Mironov, Y. V.; Virovets, A. V.; Naumov, N. G.; Ikorskii, V. N.; Fedorov, V. E. *Chem. Eur. J.* **2000**, *6*, 1361.
(23) Magliocchi, C.; Xie, X.; Hughbanks, T. *Inorg. Chem.* **2000**, *39*, 5000.
(24) Jin, S.; DiSalvo, F. J. *Chem. Commun.* **2001**, 1586.
(25) Shriver, D. F. *Struct. Bonding* **1966**, *1*, 32.
(26) Dunbar, K. R.; Heintz, R. A. *Prog. Inorg. Chem.* **1997**, *45*, 283.

10.1021/cm020103b CCC: $22.00
Published on Web 07/17/2002

strated with remarkable success and control by the Long[29−34] and Fedorov[35−39] groups. Using complexes of single metal cations as linking units, type I networks with the $[W_6S_8(CN)_6]^{6-}$ cluster anion turned out to be relatively easy to crystallize because of the dynamic and versatile coordination chemistry of the metal cations. The network structures formed with $[W_6S_8(CN)_6]^{6-}$ are (understandably) quite different from any reported network structures formed with $[Re_6Q_8(CN)_6]^{4-}$ (Q = Se, Te) and the corresponding metal ions, probably because of the different charges of the cluster anions. Even though these network structures are not expected to be electronically conducting as the electron−electron repulsion on the transition metal cations will almost certainly disrupt the electron delocalization, making the networks Mott insulators, the experience gained from studying these network linking reactions would be valuable. The proposed networks of type II incorporate other octahedral clusters, such as $\{Mo_6Cl_8\}^{4+}$ (possibly including M_6X_{12} structure types[40] as well); therefore, they might be rightfully called the "cluster analogues of Prussian Blue."[41] Nitriles are known to bind to the $\{Mo_6Cl_8\}^{4+}$ cluster,[42,43] and such linking reactions involve the axial coordination chemistry of $\{Mo_6Cl_8\}^{4+}$ clusters. Type III networks are not very likely because nitriles are not known as ligands to the W_6S_8 cluster,[6] with an exception observed in solid state.[23]

Herein, we report for the first time the synthesis, structure characterization and magnetic properties of 3-D network structures using $[W_6S_8(CN)_6]^{6-}$ and other single metal cations as building blocks. The detailed synthesis and properties of the starting $[W_6S_8(CN)_6]^{6-}$ cluster anions are included, and strategies and factors relevant to the construction of these W_6S_8 cluster network structures are discussed.

Experimental Section

General. W_6S_8(4-*tert*-butylpyridine)$_6$ was synthesized according to the reported procedure.[3] Acetonitrile and DMSO were dried with 4-Å molecular sieves and were degassed and distilled under reduced pressure. THF and diethyl ether were treated with sodium wire and distilled under reduced pressure. In-house deionized water was subjected to several freeze−pump−thaw cycles to remove the oxygen. All other reagents were used as received from commercial suppliers, including tetraethylammonium cyanide (94%) from Aldrich. Although compounds $Na_6W_6S_8(CN)_6$ (**2**)·18DMSO and $K_6W_6S_8(CN)_6$ (**3**) were reported and characterized in a preliminary report,[24] more details of the synthetic procedure are included here. The "reaction bomb" used below is a thick-walled glass vessel (i.d. = 1 in., thickness = $^1/_8$ in.) equipped with a Teflon valve and a Teflon stir bar.

^{1}H NMR and ^{13}C NMR spectra were obtained in DMSO-d_6 on a Varian VXR-400 spectrometer and were referenced to internal residual solvent resonances. Powder X-ray diffraction patterns were collected on a Scintag XDS2000 diffractometer with a flatbed sample holder or an INEL diffractometer with a capillary sample holder for any hydroscopic/air-sensitive samples. FT-IR spectra were collected with KBr pellets on a Mattson Polaris spectrometer equipped with a 4326 upgraded electronics package and a DTGS detector. Microprobe analysis was performed on a JEOL 8900R scanning electron microscope equipped with a NORAN Vantage EDS system. The thermogravimetric analyses (TGA) of the cluster complexes were done on a Seiko TG/DTA 220 thermal analyzer. The samples were loaded onto an aluminum pan and were heated from room temperature to 550 °C at a rate of 20 °C/min under a flow of dinitrogen (60 mL/min).

Syntheses. *"$(Et_4N)_5W_6S_8(CN)_6$" (1).* In a glovebox filled with argon, a reaction bomb was charged with W_6S_8(4-*tert*-butylpyridine)$_6$ (141 mg, 0.065 mmol), tetraethylammonium cyanide (Et_4NCN) (66.5 mg, 0.40 mmol, 6.16 equiv), and 10 g of DMSO. After the sealed reaction vessel was heated at 100 °C with stirring for 30 min outside of the glovebox, the initial red slurry turned into a brownish green opalescent suspension solution. The reaction mixture was filtered in the glovebox, and the resulting greenish solid was washed with copious amounts of diethyl ether. After being dried in vacuo, the fine powder product weighed 112 mg [80% yield assuming $(Et_4N)_5W_6S_8(CN)_6$ as the product].

^{1}H NMR: δ 3.22 (q, 2, α-H), 1.18 (t, 2, β-H). ^{13}C NMR: δ 52.0 (α-C), 7.5 (β-C), no free anionic CN^- (δ 166.7) compared with the spectra of Et_4NCN. IR: ν(C≡N) 2068 cm^{-1} with a shoulder around 2087 cm^{-1}. PXRD data collected using a 0.5-mm capillary are available in the Supporting Information. Two elemental analyses found: (1) C 26.34%, H 5.32%, N 6.34%; and (2) C 26.49%, H 5.10%, N 5.94%. Calculated values for $(Et_4N)_5W_6S_8(CN)_6$: C 25.5%, H 4.65%, N 7.11%. Calculated values for $(Et_4N)_6W_6S_8(CN)_6$: C 28.23%, H 5.27%, N 7.32%. Layering acetonitrile and diethyl ether subsequently on top of a filtered DMSO solution of this sample yielded dark green block-shaped single crystals on the wall of the container in 2 weeks, together with lots of tiny particles at the bottom.

$Na_6W_6S_8(CN)_6$ (2)·18DMSO. In a glovebox, a reaction bomb was charged with W_6S_8(4-*tert*-butylpyridine)$_6$ (600 mg, 0.276 mmol), NaCN (108 mg, 2.21 mmol, 8 equiv), and DMSO (10 g) to give a red slurry. The sealed reaction vessel was heated at 100 °C with stirring for 1 day outside the glovebox. Upon cooling the resulting clear dark-red solution, a large amount of crystalline particles precipitated out, which was collected by filtration in the glovebox and washed with 1 mL of DMSO and then with copious amounts of acetonitrile and diethyl ether successively. The dried dark-red granular product weighed 659 mg (78% yield). CHN analysis for **2** found (calcd): C 16.58% (16.49%), H 3.37% (3.56%), N 2.86% (2.91%). IR: ν(C≡N), 2083 cm^{-1}.

$K_6W_6S_8(CN)_6$ (3). In a glovebox, a reaction bomb was charged with W_6S_8(4-*tert*-butylpyridine)$_6$ (300 mg, 0.138 mmol), KCN (72 mg, 1.11 mmol, 8 equiv), and 6 g of DMSO. After the sealed reaction vessel was heated at 100 °C with stirring for 1 day outside the glovebox, the reaction mixture turned into a shiny opalescent suspension. The resulting solid was filtered in the

(27) Verdaguer, M.; Bleuzen, A.; Marvaud, V.; Vaissermann, J.; Seuleiman, M.; Desplanches, C.; Scuiller, A.; Train, C.; Garde, R.; Gelly, G.; Lomenech, C.; Rosenman, I.; Veillet, P.; Cartier, C.; Villain, F. *Coord. Chem. Rev.* **1999**, *190*, 1023.
(28) Ohba, M.; Okawa, H. *Coord. Chem. Rev.* **2000**, *198*, 313.
(29) Beauvais, L. G.; Shores, M. P.; Long, J. R. *Chem. Mater.* **1998**, *10*, 3783.
(30) Shores, M. P.; Beauvais, L. G.; Long, J. R. *J. Am. Chem. Soc.* **1999**, *121*, 775.
(31) Shores, M. P.; Beauvais, L. G.; Long, J. R. *Inorg. Chem.* **1999**, *38*, 1648.
(32) Beauvais, L. G.; Shores, M. P.; Long, J. R. *J. Am. Chem. Soc.* **2000**, *122*, 2763.
(33) Bennett, M. V.; Shores, M. P.; Beauvais, L. G.; Long, J. R. *J. Am. Chem. Soc.* **2000**, *122*, 6664.
(34) Bennett, M. V.; Beauvais, L. G.; Shores, M. P.; Long, J. R. *J. Am. Chem. Soc.* **2001**, *123*, 8022.
(35) Naumov, N. G.; Virovets, A. V.; Sokolov, M. N.; Artemkina, S. B.; Fedorov, V. E. *Angew. Chem., Int. Ed. Engl.* **1998**, *37*, 1943.
(36) Naumov, N. G.; Artemkina, S. B.; Virovets, A. V.; Fedorov, V. E. *Solid State Sci.* **1999**, *1*, 473.
(37) Naumov, N. G.; Artemkina, S. B.; Virovets, A. V.; Fedorov, V. E. *J. Solid State Chem.* **2000**, *153*, 195.
(38) Naumov, N. G.; Virovets, A. V.; Fedorov, V. E. *Inorg. Chem. Commun.* **2000**, *3*, 71.
(39) Naumov, N. G.; Artemkina, S. B.; Fedorov, V. E.; Soldatov, D. V.; Ripmeester, J. A. *Chem. Commun.* **2001**, 571.
(40) Prokopuk, N.; Shriver, D. F. *Adv. Inorg. Chem.* **1998**, *46*, 1.
(41) Buser, H. J.; Schwarzenbach, D.; Petter, W.; Ludi, A. *Inorg. Chem.* **1977**, *16*, 2704.
(42) Johnston, D. H.; Stern, C. L.; Shriver, D. F. *Inorg. Chem.* **1993**, *32*, 5170.
(43) Ehrlich, G. M.; Warren, C. J.; Haushalter, R. C.; DiSalvo, F. J. *Inorg. Chem.* **1995**, *34*, 4284.

Table 1. Crystallographic Data for 1 and 4−7[a]

	1	**4** (Mn)	**5** (Fe)	**6** (Co)	**7** (Zn)
chemical formula	$C_{46}H_{100}N_{11}S_8W_6$	$C_6H_{71}Mn_3N_6O_{35.5}S_8W_6$	$C_6H_{71}Fe_3N_6O_{35.5}S_8W_6$	$C_6H_{70}Co_3N_6O_{35}S_8W_6$	$C_6H_{60}K_2Zn_2N_6O_{30}S_8W_6$
formula weight	2166.95	2248.52	2267.25	2252.49	2264.64
space group	$P\bar{1}$ (No.2)	*C*2/*c* (No. 15)	*C*2/*c* (No. 15)	*C*2/*c* (No. 15)	*Pnnm* (No. 58)
a (Å)	12.056(3)	14.6782(11)	14.6008(15)	14.448(9)	15.693(2)
b (Å)	12.236(3)	22.0639(17)	21.968(2)	21.885(13)	16.914(3)
c (Å)	12.574(4)	18.4989(14)	18.286(2)	18.030(10)	11.0355(16)
α (°)	97.934(7)				
β (°)	105.571(6)	94.618(2)	94.940(6)	94.879(10)	
γ (°)	114.065(6)				
V (Å^3)	1565.6(8)	5971.6(8)	5843.6(11)	5680(6)	2929.2(8)
Z	1	4	4	4	2
refs measured	17 046	20 951	15 533	12 089	4897
unique refs	6385 (R_{int} = 0.0328)	5430 (R_{int} = 0.0411)	3027 (R_{int} = 0.0804)	3068 (R_{int} = 0.0607)	1500 (R_{int} = 0.0741)
ρ_{calcd} (g cm^{-3})	2.298	2.501	2.577	2.634	2.500
μ (cm^{-1})	112.84	124.76	128.48	133.24	130.30
R_1[b] ($I > 2\sigma$/all)	0.0321/0.0451	0.0498/0.1279	0.0459/0.0700	0.0659/0.0829	0.0555/0.1064
wR_2[c] ($I > 2\sigma$/all)	0.0624/0.0658	0.0548/0.1290	0.0773/0.0819	0.1126/0.1153	0.1064/0.1189

[a] With Mo Kα radiation (λ = 0.710 73 Å) at 173 K. [b] $R_1 = \Sigma||F_o| - |F_c||/\Sigma|F_o|$. [c] $wR_2 = [\Sigma w(F_o^2 - F_c^2)^2/\Sigma w(F_o^2)^2]^{1/2}$.

glovebox and washed with 1 mL of DMSO and copious amounts of acetonitrile and diethyl ether subsequently. The dried lustrous gray powder weighed 220 mg (90% yield). CHN analysis for **3**: found (calcd) C 6.48% (4.13%), H 0.58% (0%), N 4.77% (4.78%). IR: ν(C≡N), 2038 cm^{-1}.

$[Mn(H_2O)_4]_3[W_6S_8(CN)_6]\cdot 23.5H_2O$ (4). Under a blanket of argon, $Na_6W_6S_8(CN)_6$ (**2**)·18 DMSO (201 mg, 0.065 mmol) was dissolved in 10 mL of deoxygenated water in a 100-mL Schlenk flask to give a clear brown-red solution. A 15-mL water solution of $MnSO_4\cdot 5H_2O$ (63 mg, 0.261 mmol) was carefully layered on top of the cluster solution under argon flow. The sealed flask was stored in a refrigerator for 3 days to produce a large amount of stick-like brown-red crystals and a lightly colored solution. The solid was collected by filtration and washed with 3 × 5 mL of water to yield 131 mg of product (86% yield). Microprobe analysis on heavier elements found (calcd): Mn 11.4% (10.8%), W 71.0% (72.4%), S 17.6% (16.8%). IR: ν(C≡N), 2089 cm^{-1}.

$[Fe(H_2O)_4]_3[W_6S_8(CN)_6]\cdot 23.5H_2O$ (5). Procedures analogous to those for **4** were carried out with 300 mg (0.098 mmol) of **2**·18DMSO, $FeCl_2\cdot 4H_2O$ (78 mg, 0.39 mmol), and a total of 30 mL of water with an immediate precipitation of a cloudy brown-yellowish solid. After 2 days in the refrigerator, this suspension turned into tiny crystalline particles settled at the bottom of a colorless solution. The brown-red solid was filtered and washed with water to yield 180 mg of product (78% yield). Microprobe analysis on heavier elements found (calcd): Fe 12.1% (11.0%), W 70.1% (72.2%), S 17.8% (16.8%). IR: ν(C≡N), 2086 cm^{-1}.

$[Co(H_2O)_4]_3[W_6S_8(CN)_6]\cdot 23H_2O$ (6). Procedures analogous to those for **4** were carried out with 100 mg (0.046 mmol) of **2**·18DMSO, $Co(NO_3)_2\cdot 6H_2O$ (38 mg, 0.13 mmol), and a total of 15 mL of water to yield an immediate precipitation of a cloudy brown-yellowish solid, which turned into tiny crystalline particles in a colorless solution after 1 week in the refrigerator. The brown-red solid was filtered and washed with water to yield 59 mg of product (78% yield). Microprobe analysis on heavier elements found (calcd): Co 10.7% (11.5%), W 72.0% (71.8%), S 17.3% (16.7%). IR: ν(C≡N), 2088 cm^{-1}.

$Na_2[Zn(H_2O)_2]_2[W_6S_8(CN)_6]\cdot 26H_2O$ (7). Analogous procedures to those for **4** were carried out with 150 mg (0.069 mmol) of **2**·18DMSO, $Zn(NO_3)_2\cdot 6H_2O$ (44 mg, 0.15 mmol), and a total of 40 mL of water to yield an immediate precipitation of a light yellow solid, which did not change much over 1 week in the refrigerator. The resulting muddy light brown-yellow solid was filtered and washed with water to yield 112 mg of product (84% yield). Microprobe analysis on heavier elements found (calcd): Na 3.4% (3.0%) Zn 8.7% (8.5%), W 71.1% (71.8%), S 17.1% (16.7%). IR: ν(C≡N), 2091 cm^{-1}.

X-ray Structure Determination. The single crystals of compounds **4**−**7** were grown by diffusing dilute aqueous solutions of the two reactants in narrow diameter tubes placed in a refrigerator for several days. Additional water buffer layers had to be added for **6** and **7** to slow the diffusion and acquire sufficiently large crystals. The single crystals of **7** were grown with $K_6W_6S_8(CN)_6$ (**3**) as the starting material for the better differentiation of K^+ from water molecules in structural refinements. The crystals are hydroscopic (**1**) or efflorescent (**4**−**7**); therefore, when removed from the mother liquors, they were immediately immersed in polybutene oil, and the single crystals were quickly selected and immediately placed in a cold dinitrogen stream. X-ray diffraction data were collected on a Bruker SMART system with a CCD detector using Mo Kα radiation at 173 K. The cell constants were determined from more than 50 well-centered reflections. The data were integrated using SAINT software,[44] and empirical absorption corrections were applied using the SADABS program (*β* revision).[45] The space groups were determined on the basis of systematic absences, intensity statistics, and the successful refinements of the structures. The structures were solved using SHELXS[46] with direct methods to reveal the positions of W and S atoms. Difference Fourier syntheses following the subsequent full-matrix least-squares refinements on F_o^2 with SHELXL software packages revealed the ligand atoms and other heavier atoms. Only the hydrogen atoms in **1** were assigned to the ideal positions and refined using a riding model. The tetraethylammonium (Et_4N^+) cation sitting on an inversion center in structure **1** was disordered and modeled successfully. All non-hydrogen atoms in structure **1** were refined anisotropically. In the network structures (**4**−**7**), however, only the cluster core (W and S) atoms, the M(II) cations, and the coordinated water oxygen atoms were refined anisotropically. The large number of waters of crystallization always present in the network structures (**4**−**7**) were often disordered and were refined with variables occupancies. Final refinements converged, and the residual electron densities were near the heavy atoms (W and M). The crystallographic data are summarized in Table 1. A polymorph of $(Et_4N)_5W_6S_8(CN)_6$ (**1**) was also observed in a rhombahedral $R\bar{3}c$ (No. 167) space group with a = 12.843(1) Å and c = 67.617(5) Å. Even though the chemical composition was shown to be the same, the structure was not refined to satisfactory R factors because of the poor data quality.

Magnetic Susceptibility. In a glovebox, a gelcap containing 35 mg of **1** was inserted into a straw, which was then placed into a Quantum Design SQUID magnetometer with

(44) *SAINT Plus, Software for the CCD Detector System*; Bruker Analytical X-ray System: Madison, WI, 1999.

(45) Sheldrick, G. M. *SADABS Siemens Area Detector Absorption Correction Program*; Institute für Anorganische Chemie der Universität Göttingen: Göttingen, Germany, 1999.

(46) Sheldrick, G. M. *SHELXL*, version 5.10; Siemens Analytical X-ray Instruments Inc.: Madison, WI, 1999.

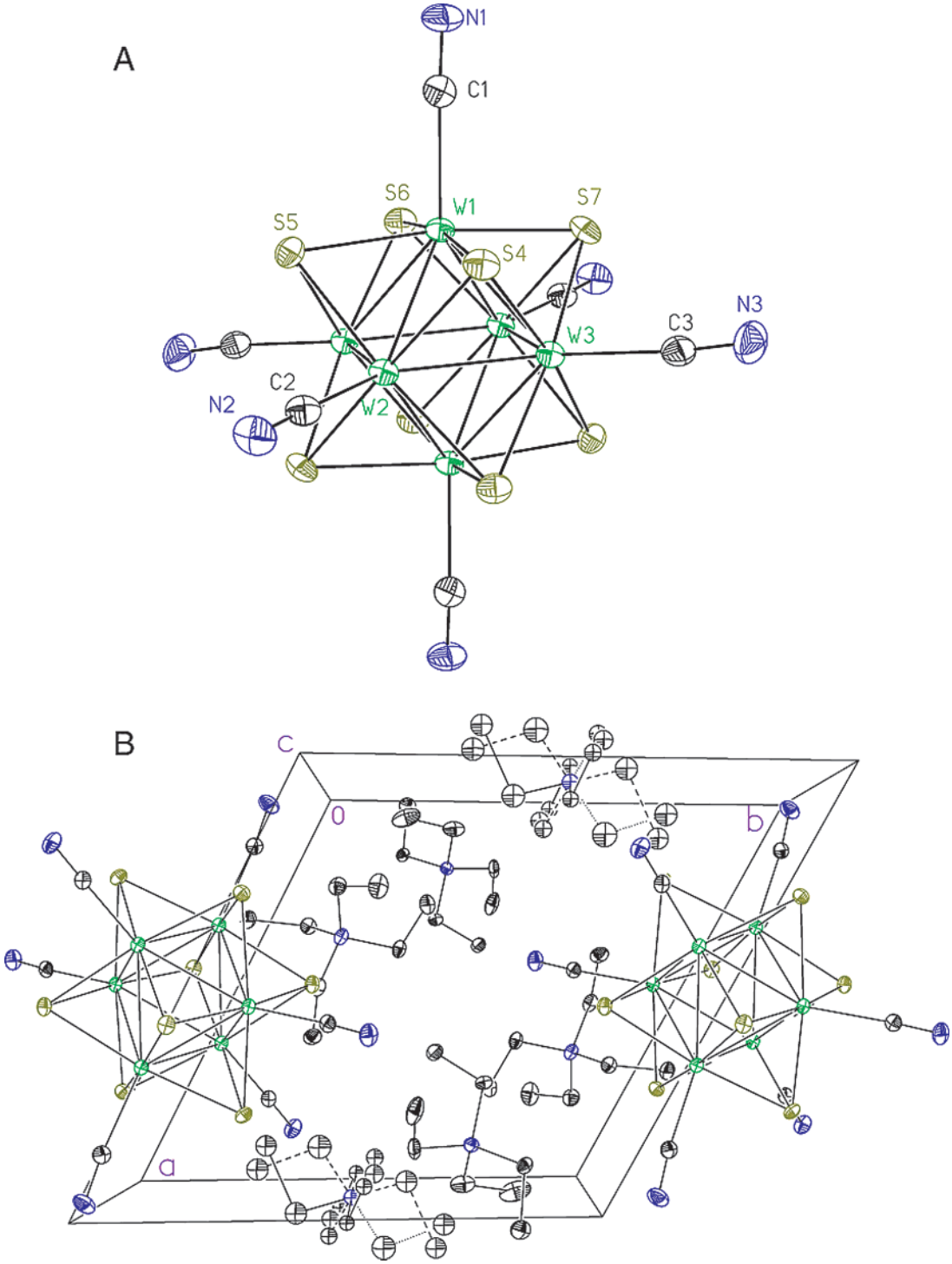

Figure 1. Crystal structure of $(Et_4N)_5W_6S_8(CN)_6$ (**1**): (A) ORTEP diagram of the $[W_6S_8(CN)_6]^{5-}$ cluster anion at 50% probability, (B) packing diagram of $(Et_4N)_5W_6S_8(CN)_6$ along the *c* axis showing the disorder of Et_4N^+ cation on inversion center.

minimal exposure to air. Magnetic susceptibility measurements were performed over the temperature range 6−300 K with an applied field of 7000 Oe. A sample of 52 mg of $[Fe(H_2O)_4]_3[W_6S_8(CN)_6]\cdot 23.5H_2O$ (**5**) was prepared similarly but in the air, and the magnetic susceptibility measurements were performed over the temperature range 4−300 K with an applied field of 6000 Oe. The susceptibilities at 5 and 300 K as a function of field (500−29 500 Oe) were also measured to check for ferromagnetic impurities. The data were corrected for the diamagnetic gelcap contributions and also for the diamagnetic core contributions (-1.00×10^{-3} emu/mol for **1** and -0.95×10^{-3} emu/mol for **5**) that were calculated from values for the individual atoms.[47]

Results and Discussion

Synthesis and Properties of the Octahedral Tungsten Sulfidocyanide Cluster Anion. As demonstrated in the preliminary report,[24] $[W_6S_8(CN)_6]^{6-}$ can be prepared by ligand exchange with W_6S_8(4-*tert*-butylpyridine)$_6$, as shown in eq 1. The most convenient procedure is reacting NaCN with W_6S_8(4-*tert*-butylpyridine)$_6$ in DMSO solvent. The unexpected solubility of

(47) Selwood, P. W. *Magnetochemistry*, 2nd ed.; Interscience: New York, 1956; p 78.

Table 2. Selected Bond Lengths (Å) and Angles (°) for $(Et_4N)_5W_6S_8(CN)_6$ (1) and $Na_6W_6S_8(CN)_6$ (2) Compounds in Comparison with $W_6S_8(t\text{-BuNC})_6$[a]

cluster	$(Et_4N)_5W_6S_8(CN)_6$ (**1**)	$Na_6W_6S_8(CN)_6$ (**2**)	$W_6S_8(t\text{-BuNC})_6$
W−W	2.6882(6)−2.7256(7)	2.6817(4)−2.6875(4)	2.6776(5)−2.6870(5)
mean[a]	2.697(13)	2.685(2)	2.681(3)
δ_{W-W}[b]	0.0374	0.0058	0.0094
W−S	2.431(2)−2.478(2)	2.4518(15)−2.4667(11)	2.443(2)−2.456(2)
mean[a]	2.454(13)	2.459	2.450(5)
δ_{W-S}[b]	0.047	0.0149	0.013
W−W−W[c]	89.257(15)−90.743(15)	90	89.896(15)−90.105(15)
δ_{W-W-W}[b]	1.486		0.209
W−W−W[d]	59.485(14)−60.86(2)	59.855(12)−60.073(5)	59.882(13)−60.151(14)
δ_{W-W-W}[b]	1.375	0.218	0.269
W−C	2.189(7)−2.212(6)	2.196(5)	2.146(9)−2.169(9)
mean[a]	2.197(7)	2.196(5)	2.160(10)

[a] Followed by standard deviations (σ) of the group of bond lengths in parentheses. $\sigma = [\Sigma(d_j - d_m)^2/n]^{1/2}$. The data for $W_6S_8(t\text{BuNC})_6$ are from ref 6. [b] Maximum deviations. [c] Within equatorial squares. The mean W−W−W angles within the equatorial squares are automatically 90° when the clusters have inversion centers. [d] Within triangular faces. The mean angles are 60° by geometry

$Na_6W_6S_8(CN)_6$ [quite soluble in hot DMSO, but only slightly soluble in DMSO at room temperature (RT)] simplifies the isolation of the *brown-red* crystalline product of $Na_6W_6S_8(CN)_6$ (**2**)·18DMSO.

$$W_6S_8(4\text{-}tert\text{-butylpyridine})_6 + > 6\ M^+CN^- \xrightarrow{\Delta} M_6W_6S_8(CN)_6 + 6(4\text{-}tert\text{-butylpyridine}) \quad M = Na, K \quad (1)$$

However, initial solubility considerations led us to use Et_4NCN, an organic cyanide salt, to react with W_6S_8(4-*tert*-butylpyridine)$_6$ or other $W_6S_8L_6$ clusters, producing a perplexing *greenish* crystalline powder. Although bound 4-*tert*-butylpyridine ligand and free cyanide were absent in the NMR spectrum for the solution of this sample while Et_4N^+ cation was present, the composition could not be confirmed to be $(Et_4N)_6W_6S_8(CN)_6$, as the ^{13}C NMR signal from the bound cyanide ligand could not be observed. CHN analysis results also showed significant deviations from the expected values for $(Et_4N)_6W_6S_8(CN)_6$. X-ray structural analysis of the *green* block-shaped single crystals grown from this powder established a surprising composition of $(Et_4N)_5W_6S_8(CN)_6$ (vide infra), i.e., the cluster anion was oxidized by one electron from the starting W_6S_8(4-*tert*-butylpyridine)$_6$ cluster. The presence of paramagnetic species was confirmed by the magnetic measurement. Yet, neither the magnetic measurement nor the powder diffraction pattern (both available in the Supporting Information) show that the product consists of pure $(Et_4N)_5W_6S_8(CN)_6$. Indeed, there were seemingly different products that resulted from the recrystallization. The analyzed single crystals were merely selective crystallization from a mixture. It was concluded that in the ligand exchange reactions with Et_4NCN, at least a portion of the cluster was oxidized by unidentified reagent(s) (possibly in the commercial Et_4NCN). Fortunately, using NaCN or KCN, the unoxidized $[W_6S_8(CN)_6]^{6-}$ cluster anion can be conveniently synthesized and verified. No further improvements of the reaction using Et_4NCN were attempted. Nonetheless, this crystallization of the oxidized $(Et_4N)_5W_6S_8(CN)_6$ cluster might be useful for characterization and isolation of the oxidized cluster anion if so desired. ^{13}C NMR spectroscopy showed that $[W_6S_8(^{13}CN)_6]^{6-}$ is stable in deoxygenated water,[24] which paved the way for the network-building reactions described below.

Structures of the Octahedral Tungsten Sulfidocyanide Cluster Anions. The structure for the selectively crystallized *green* single crystals was determined and shown in Figure 1. Six cyanide groups bind as the axial ligands to the familiar[6] octahedral W_6S_8 cluster core. The composition of this structure is $(Et_4N)_5W_6S_8(CN)_6$ because a disordered Et_4N^+ cation resides on an inversion center of the lattice (Figure 1B), resulting in a maximum of five Et_4N^+ cations per cluster anion. Some selected bond lengths and angles for structure **1** are collected in Table 2 and compared with those of unoxidized $Na_6W_6S_8(CN)_6$ (**2**)[24] and neutral $W_6S_8(t\text{-BuNC})_6$[6] structures. The 19-electron $[W_6S_8(CN)_6]^{5-}$ cluster anion is quite irregular compared with the analogous 20-electron clusters. The average W−W bond length in **1**, 2.697(13) Å, is slightly longer than those in the unoxidized structures, in accordance with the previous studies of the oxidized $[W_6S_8(PEt_3)_6]^+$ cluster cation.[5]

Syntheses of the Cluster Networks. Reacting deoxygenated aqueous solutions of transition metal salts, such as Mn^{2+}, Fe^{2+}, Co^{2+} and Zn^{2+}, with deoxygenated aqueous solutions of the $[W_6S_8(CN)_6]^{6-}$ cluster anion at room temperature produced crystalline products $[M^{(II)}(H_2O)_4]_3[W_6S_8(CN)_6]\cdot xH_2O$ [$x \approx 23$; M = Mn (**4**), Fe (**5**), Co (**6**)] and $Na_2[Zn(H_2O)_2]_2[W_6S_8(CN)_6]\cdot xH_2O$ (**7**). The reactions are

$$3[M(H_2O)_6]^{2+} + [W_6S_8(CN)_6]^{6-} \rightarrow [M^{(II)}(H_2O)_4]_3[W_6S_8(CN)_6]\cdot xH_2O \quad [x \approx 23;\ M = Mn\ (\mathbf{4}),\ Fe\ (\mathbf{5}),\ Co\ (\mathbf{6})] \quad (2)$$

$$2[Zn(H_2O)_6]^{2+} + Na_6[W_6S_8(CN)_6]^{6-} \rightarrow Na_2[Zn(H_2O)_2]_2[W_6S_8(CN)_6]\cdot xH_2O\ (x \approx 26) + 4\ Na^+ \quad (3)$$

The formation of the products is insensitive to the stoichiometry of the reagents, as single crystals were grown with various ratios and concentrations for the optimal crystal quality for X-ray analysis. In the bulk syntheses, slight excesses of the metal salts were used to produce essentially quantitative yields (the less than 100% yields are attributed to transfer losses). The ν-(C≡N) bands in the IR spectra of the products (**4**−**7**) shift to slightly higher frequencies from those of the starting material (**2**). The choices of anions for the

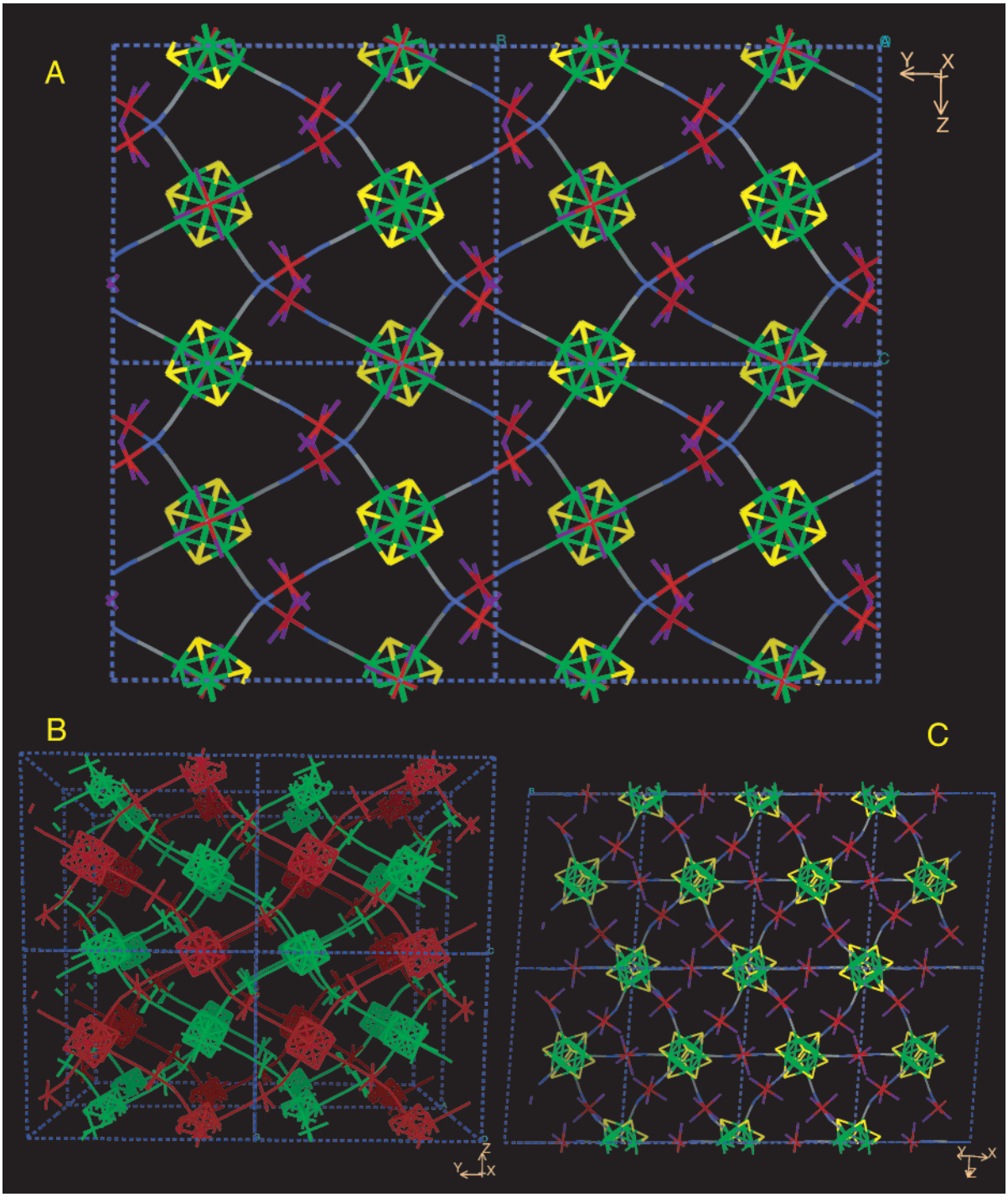

Figure 2. Network structure of $[M(H_2O)_4]_3[W_6S_8(CN)_6]\cdot xH_2O$ ($x \approx 23$; M = Mn, Fe, Co) using M = Fe (**5**) as an example: (A) along the *a* axis; (B) perspective view along the *a* axis showing the two interpenetrating networks in different colors; (C) roughly along the pseudo-3-fold axis of the cluster. Color code for A and C: green, W; yellow, S; gray, C; blue, N; red, Fe; cyan, O.

starting transition metal salts (Cl^-, SO_4^{2-}, or NO_3^-, etc.) and the countercations for $[W_6S_8(CN)_6]^{6-}$ (K^+ or Na^+) are not important, as almost identical crystal sizes, morphologies, and cell parameters were persistently observed. At least for reaction 2, this can be explained by the exclusion of countercations in the neutral network products. The difficulty of crystallization increases from Mn to Zn, with Fe and Co seemingly going through some less crystalline intermediate stages, and Zn causes instantaneous precipitation. We have not yet been able to obtain any crystalline products using other 3d metal ions (vide infra).

3-D Structures of the Cluster Networks. X-ray structural analyses on the single crystals grown by careful diffusion revealed two 3-D structural types as the products of the reactions above: $[M^{(II)}(H_2O)_4]_3[W_6S_8(CN)_6]\cdot xH_2O$ [$x \approx 23$; M = Mn (**4**), Fe (**5**), Co (**6**)] and $K_2[Zn(H_2O)_2]_2[W_6S_8(CN)_6]\cdot 26H_2O$ (**7**).

The network structure of $[M(H_2O)_4]_3[W_6S_8(CN)_6]\cdot xH_2O$ ($x \approx 23$; M = Mn, Fe, Co) is displayed in Figure 2 using M = Fe (**5**) as an example because all three (**4**–**6**) are isostructural. The structure consists of two identical interpenetrating 3-D distorted cubic networks that are made up of octahedral-coordinated $[W_6S_8(CN)_6]^{6-}$

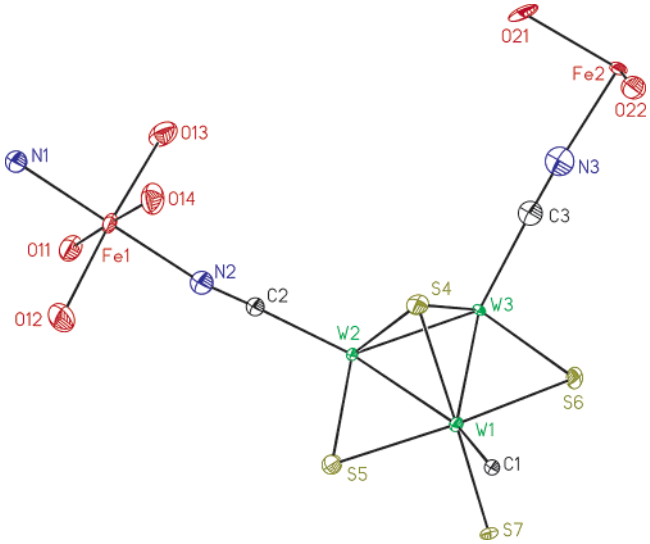

Figure 3. Local structure in $[M(H_2O)_4]_3[W_6S_8(CN)_6]\cdot xH_2O$ ($x \approx 23$; M = Mn, Fe, Co) using M = Fe (**5**) as an example: ORTEP diagram of the asymmetric unit at the 30% probability level.

cluster anions and effectively ditopic −CN−[*trans*-Fe-$(H_2O)_4$]−NC− bridges. Each cluster anion bonds through six axial cyanide ligands to six Fe(II) complexes, and each Fe(II) ion bonds to two N terminals of the cyanides in trans fashion, while its octahedral coordination environment is completed by four additional water molecules in the equatorial plane. The local environment can be better viewed in Figure 3 where the asymmetric unit of this structure is shown. $[W_6S_8(CN)_6]^{6-}$ and one Fe atom (Fe2) reside on inversion centers of the lattice, while Fe1 resides on a general position and bonds to two independent N atoms (N1 and N2). Such linkage leads to a 3:1 ratio of divalent metal ions to $[W_6S_8(CN)_6]^{6-}$ cluster anions, resulting in a neutral α-Po-like simple cubic network.[48,49] Because the octahedral cluster nodes of this net are connected through a rather long W−CN-M-NC−W bridge, this network is very open: the cubic edges are roughly 14.4 Å, longer than those found in the reported $[Re_6Q_8(CN)_6]^{4-/3-}$ cluster networks.[29−39] Because of this fairly large dimension, interpenetration occurs to "eliminate the vacuum".[50] Shown in green and red colors in Figure 2B to highlight the interpenetration, one network resides roughly in the "body center" of the other identical network (in fact, the two are related with the *C* centering of the lattice). The potential interference between the coordinated water molecules on the crossing Fe centers might cause the aesthetically pleasing wiggling pattern on the *bc* plane (the bridge is essentially collinear along the *a* axis).

Figure 4 displays the completely different structure of $K_2[Zn(H_2O)_2]_2[W_6S_8(CN)_6]\cdot 26H_2O$ (**7**). Here, the octahedral $[W_6S_8(CN)_6]^{6-}$ cluster anion still bonds to six Zn(II) ions through the axial cyanide ligands, but Zn(II) is in a trigonal bipyramidal coordination mode with three N terminals of cyanide on the equatorial plane and two water molecules in axial positions (see the local structure in Figure 5). The five-coordinated Zn(II) complex is rather rare but not without precedent.[51] This effectively creates a rutile (TiO_2) net,[48,49] with clusters corresponding to the octahedral Ti nodes and Zn complexes corresponding to the trigonally coordinated O nodes. Rutile nets in coordination networks were observed before but with interpenetration.[52] The overall charge for the network is −2, so there are two K^+ cations located in the cavities close to the cluster.

The cavities of both structural types are filled with a large number of disordered water molecules, as is the case for other cluster network compounds.[29−39] The water composition was proposed purely on the basis of crystallographic refinements because the crystals readily lose water (vide infra) and the exact water content is difficult to determine. In both structural motifs (**4**−**7**), cyanide groups are believed to be bound to the W with C terminals, not only because of the structure refinements but also because the CN^- group is kinetically inert on W_6S_8 at RT according to our NMR spectroscopic study. The cyanide group is verified to coordinate to W via the C terminal in the starting clusters.[24] Selected interatomic distances and angles are collected in Table 3 for all network structures (**4**−**7**). The W−C distances in the network structures are *slightly* shorter than those in isolated cluster anions, as are the W−W distances. The cluster cores are by and large regular and rather unaffected by the networks.

Unsuccessful Network-Building Attempts with $[W_6S_8(CN)_6]^{6-}$. Unsuccessful linking reactions using $[W_6S_8(CN)_6]^{6-}$ with other transition metal ions in water, transition metal salts (including some of the metal ions above) or $\{Mo_6Cl_8\}^{4+}$ clusters in dry DMSO ("type II" network construction), and other $W_6S_8L_6$ clusters ("type III" network) are listed in Table S1 of the Supporting Information. These reactions invariably led to precipitates but failed to produce crystalline materials or crystals sufficiently large for X-ray structure analysis despite similar efforts at crystal growth.

It can be readily noticed that, among the network structures linked with metal clusters[29−39,53,54] or clusters in the broad sense,[55−62] the linking reaction invariably occurs around the single metal coordination centers instead of in the cluster coordination environment. We have been trying to construct extended structures with

(48) O'Keeffe, M.; Eddaoudi, M.; Li, H.; Reineke, T.; Yaghi, O. M. *J. Solid State Chem.* **2000**, *152*, 3.
(49) Robson, R. *J. Chem. Soc., Dalton Trans.* **2000**, 3735.
(50) Batten, S. R.; Robson, R. *Angew. Chem., Int. Ed. Engl.* **1998**, *37*, 1461.
(51) Venkataraman, D.; Du, Y.; Wilson, S. R.; Hirsch, K. A.; Zhang, P.; Moore, J. S. *J. Chem. Educ.* **1997**, *74*, 915.
(52) Batten, S. R.; Hoskins, B. F.; Moubaraki, B.; Murray, K. S.; Robson, R. *J. Chem. Soc., Dalton Trans.* **1999**, 2977.
(53) Fedin, V. P.; Virovets, A. V.; Kalinina, I. V.; Ikorskii, V. N.; Elsegood, M. R. J.; Clegg, W. *Eur. J. Inorg. Chem.* **2000**, 2341.
(54) Mironov, Y. V.; Virovets, A. V.; Sheldrick, W. S.; Fedorov, V. E. *Polyhedron* **2001**, *20*, 969.
(55) Zhang, S.-W.; Wei, Y.-G.; Yu, Q.; Shao, M.-C.; Tang, Y.-Q. *J. Am. Chem. Soc.* **1997**, *119*, 6440.
(56) Liu, G.; Wei, Y.-G.; Yu, Q.; Liu, Q.; Zhang, S.-W. *Inorg. Chem. Commun.* **1999**, *2*, 434.
(57) Muller, A.; Krickemeyer, E.; Bogge, H.; Schmidtmann, M.; Beugholt, C.; Das, S. K.; Peters, F. *Chem. Eur. J.* **1999**, *5*, 1496.
(58) Khan, M. I.; Yohannes, E.; Doedens, R. J. *Angew. Chem., Int. Ed.* **1999**, *38*, 1292.
(59) Khan, M. I.; Yohannes, E.; Powell, D. *Chem. Commun.* **1999**, 23.
(60) Khan, M. I.; Yohannes, E.; Powell, D. *Inorg. Chem.* **1999**, *38*, 212.
(61) Khan, M. I. *J. Solid State Chem.* **2000**, *152*, 105.
(62) Hagrman, P. J.; Finn, R. C.; Zubieta, J. *Solid State Sci.* **2001**, *3*, 745.

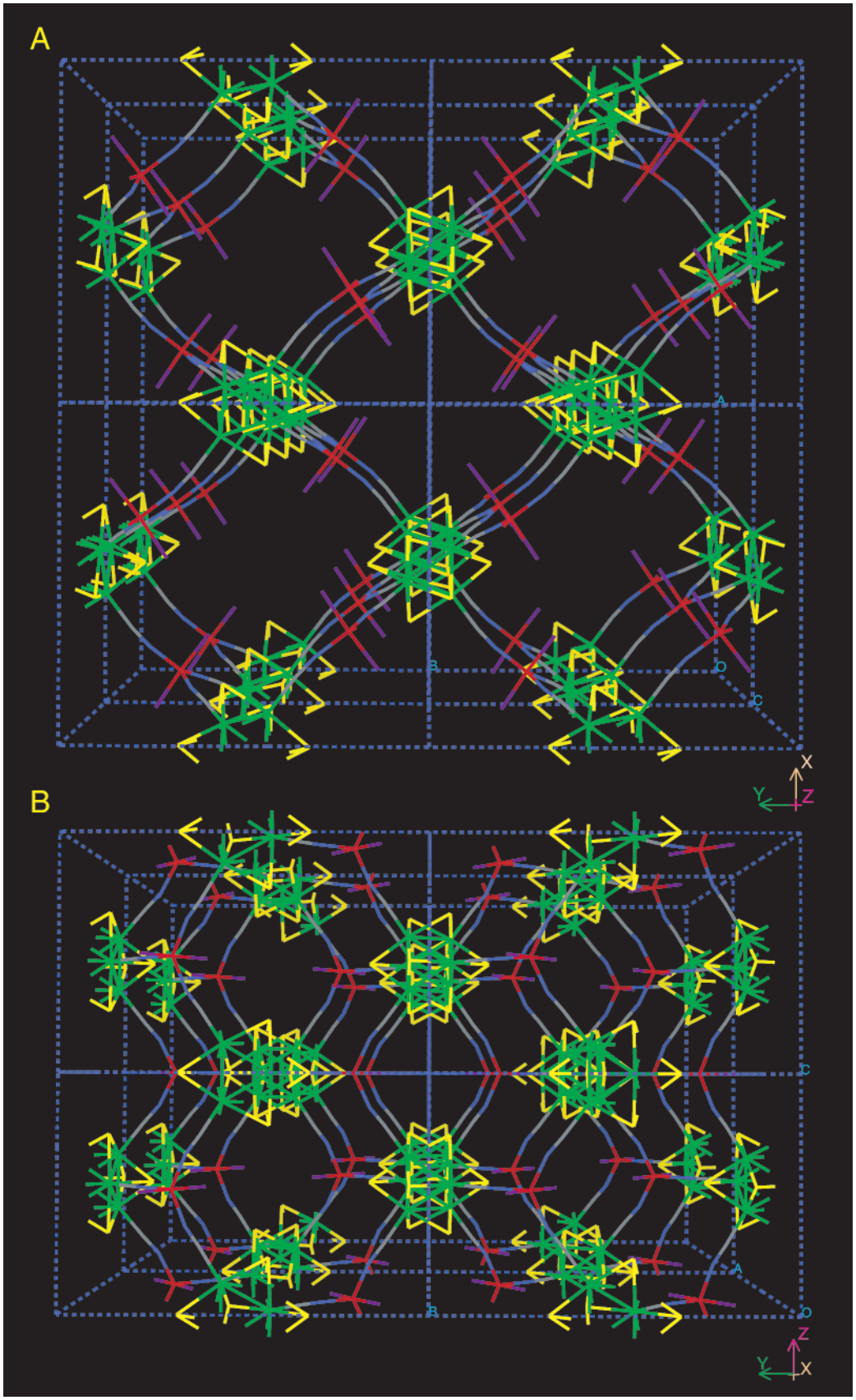

Figure 4. Network structure of $K_2[Zn(H_2O)_2]_2[W_6S_8(CN)_6]\cdot 26H_2O$ (**7**): (A) along the *c* axis; (B) along the *a* axis. Color code: green, W; yellow, S; gray, C; blue, N; red, Zn; cyan, O.

the W_6S_8 clusters and π-conjugated ditopic ligands in hopes of producing materials with interesting electronic properties. We found that *directly* linking these octahedral clusters with neutral ditopic organic ligands is plagued by the poor crystallinity and insolubility of the obtained network or oligomeric products.[63] The same difficulties have been encountered by Shriver and coworkers in linking $\{Mo_6Cl_8\}^{4+}$ clusters with neutral

Table 3. Selected Bond Lengths (Å) and Angles (°) for Network Structure Compounds $[M^{(II)}(H_2O)_4]_3[W_6S_8(CN)_6]\cdot xH_2O$ [$x \approx 23$; M = Mn (4), Fe (5), Co (6)] and $K_2[Zn(H_2O)_2]_2[W_6S_8(CN)_6]\cdot 26H_2O$ (7)[a]

compound (M)	**4** (Mn)	**5** (Fe)	**6** (Co)	**7** (Zn)
W−W	2.6718(6)−2.6795(6)	2.6752(10)−2.6802(10)	2.6628(16)−2.6822(19)	2.664(2)−2.6754(19)
mean[a]	2.676(3)	2.677(2)	2.672(6)	2.672(4)
δ_{W-W}[b]	0.0077	0.005	0.0194	0.011
W−S	2.455(3)−2.470(3)	2.446(5)−2.470(5)	2.443(6)−2.474(6)	2.444(11)−2.468(7)
mean[a]	2.461(4)	2.457(7)	2.458(9)	2.457(8)
W−W−W[c]	89.77(2)−90.23(2)	89.87(3)−90.13(3)	89.59(6)−90.41(6)	89.86(6)−90.14(6)
W−W−W[d]	59.86(2)−60.18(2)	59.89(3)−60.11(3)	59.71(4)−60.43(5)	59.77(6)−60.14(5)
W−C	2.177(11),2.152(10),2.165(13)	2.180(16), 2.162(17),2.16(2)	2.17(2), 2.12(2), 2.12(3)	2.04(4), 2.16(3)
C−N	1.154(15), 1.177(15), 1.142(19)	1.155(18), 1.145(19), 1.160(20)	1.15(2), 1.17(3), 1.15(3)	1.26(4), 1.15(3)
W−C−N	172.3(10), 179.4(11), 178.3(18)	175.4(14), 177.2(15), 178.2(18)	174(2), 174(2), 178(2)	174(4), 176(2)
M−N	2.157(10), 2.174(10), 2.149(16)	2.116(14), 2.129(15), 2.099(19)	2.09(2), 2.09(2), 2.09(2)	1.95(2), 1.96(2)
C−N−M	164.9(10), 172.8(11), 174.5(19)	163.2(14), 168.9(15), 175.1(18)	163.3(19), 177(2), 172(2)	172(3), 166(2)
M−O	2.18(1)−2.24(1)	2.108(14)−2.191(15)	2.09(2)−2.144(19)	2.25(3)−2.25(3)
mean[a]	2.21(2)	2.16(3)	2.12(2)	2.25(3)
N−M−N	176.3(5)	176.1(5)	175.4(8)	119.7(6), 120.6(12)
N−M−O	86.7(5)−92.7(4)	87.8(5)−92.4(5)	87.9(9)−92.3(7)	86.7(5)−92.7(4)
mean[a]	90.0(1.8)	90.0(1.6)	90.0(1.4)	90.0(2.1)
O−M−O	87.6(4)−95.3(6)	88.1(5)−91.4(6)	88.6(8)−92.9(8)	176.9(9)
mean[a]	90.0(3.5)	90.0(1.3)	90.0(1.9)	176.9(9)

[a] Followed by standard deviations (σ) of the group of bond lengths in parentheses. $\sigma = [\sum(d_j - d_m)^2/n]^{1/2}$. [b] Maximum deviations. [c] Within equatorial squares. The mean W−W−W angles within the equatorial squares are automatically 90° if the clusters have inversion centers. [d] Within triangular faces. The mean angles are 60° by geometry.

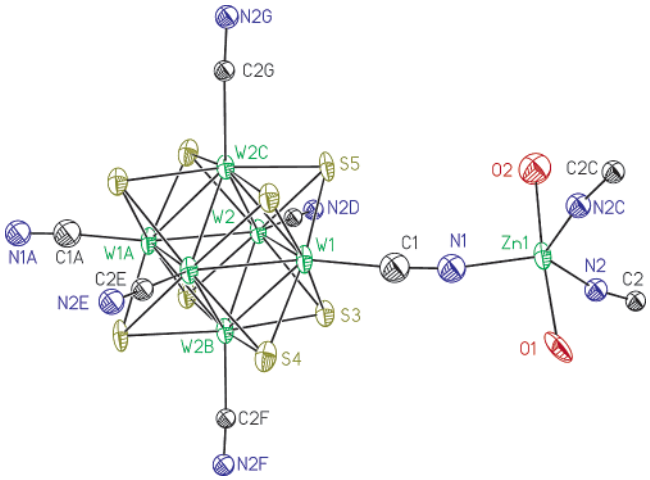

Figure 5. Local structure in $K_2[Zn(H_2O)_2]_2[W_6S_8(CN)_6]\cdot 26H_2O$ (**7**): ORTEP diagram of the cluster and the Zn complex at the 30% probability level.

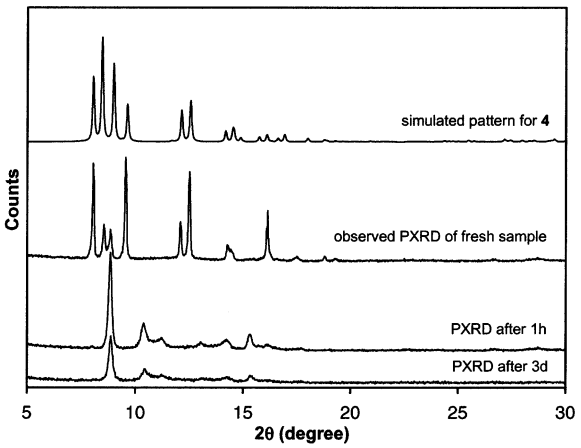

Figure 6. Evolution of the powder X-ray diffraction patterns of $[Mn(H_2O)_4]_3[W_6S_8(CN)_6]\cdot 23.5H_2O$ (**4**) in air at RT in comparison with the diffractogram calculated from the crystal structure.

ligands.[64] Comparing these cases, perhaps the fast coordination kinetics of 3d transition metal ions facilitate a dynamic recrystallization crucial to the organization of "supramolecular" structures.[65,66] Incorporating various number of water molecules and adopting different coordination motifs, these metal ions also serve as the "wild cards" of the structure components, as witnessed in the structural varieties of the octahedral cyanide cluster networks. The different results caused by using DMSO or water as the solvent might illustrate the critical role played by water as a competing ligand. It can be generalized that *crystalline* network structures incorporating single metal cations can be synthesized without much elaboration as nature can always find a way around their coordination chemistry. From a broader perspective, the intensive efforts in constructing network structures[48−50,67,68] mostly concern the structural type predictions on the basis of the geometry of the building blocks,[48,49] presuming that crystalline structures can form. Perhaps the typical research approach was best described by Robson:[69] "We were mindful of the distinct risk that such polymerizing systems could lead to irregular linking up of units, giving amorphous materials of indefinite composition (e.g., with many "loose ends"). Nevertheless, the probability that ordered, truly crystalline structures might spontaneously assemble appeared to us sufficiently high to make some trial syntheses worthwhile." As a result, many more networks that are not so readily *crystallized* were ignored and few were concerned with the mechanism of the network crystallization,[70] the critical insights on the differences between the crystalline and amorphous linking reactions were not gained. Although adhering

(63) Rayburn, L. L. Ph.D. Thesis, Cornell University, Ithaca, NY, 2000.
(64) Bain, R. L.; Shriver, D. F.; Ellis, D. E. *Inorg. Chim. Acta* **2001**, *325*, 171.
(65) Lehn, J.-M. *Pure Appl. Chem.* **1994**, *66*, 1961.
(66) Lehn, J.-M. *Supramolecular Chemistry: Concepts and Perspectives*; VCH Publishers: Weinheim, Germany, 1995.
(67) For examples, see special issues of *J. Solid State Chem.* **2000**, *152* (1), and *J. Chem. Soc., Dalton Trans.* **2000**, (21).
(68) Moulton, B.; Zaworotko, M. J. *Chem. Rev.* **2001**, *101*, 1629.
(69) Hoskins, B. F.; Robson, R. *J. Am. Chem. Soc.* **1990**, *112*, 1546.
(70) Carlucci, L.; Ciani, G.; Moret, M.; Proserpio, D. M.; Rizzato, S. *Chem. Mater.* **2002**, *14*, 12.

to the crystal producing systems certainly led to great progress in collecting and categorizing network structures, perhaps understanding those systems devoid of crystalline networks will truly shed light on the "*synthesis*" of the coordination network structures.

Stability of the Network Structures Compounds. The powder diffraction patterns of the network structures (**4**−**7**) change quickly in air even at RT. An example for compound **4** is shown in Figure 6. The peak positions of the PXRD pattern for the fresh sample out of the mother liquor matched well with those of the calculated pattern from single-crystal data (the differences in peak intensities are due to the preferred orientation and small number of rod-shaped fragile crystals), but after 1 h, it was completely different from the original pattern, and the crystallinity slowly diminished with time. Thermogravimetric analyses (TGA) of **4**−**7** showed that they all start to lose water of crystallization at RT and that the weight losses are stabilized around 100 °C and are not significantly different up to 550 °C. The total weight losses varied from 36 to 23% of the initial weights for different compounds. This reflects the different degrees of water loss before the TGA experiments, underlining how readily these compounds decay, even though the analyses were performed as promptly as possible after the samples were isolated. In conclusion, in contrast to some fairly robust porous structures observed in the $[Re_6Q_8(CN)_6]^{4-/3-}$ cluster networks, the fragile structures herein irreversibly change as they lose water of crystallization, making them unsuitable for sorption/desorption applications.

Magnetic Properties of 5. The magnetic susceptibility for $[Fe^{(II)}(H_2O)_4]_3[W_6S_8(CN)_6]\cdot xH_2O$ ($x \approx 23$) (**5**) over the temperature range 4−300 K (shown in Figure S3 in the Supporting Information) is well described by the Curie−Weiss relation, $\chi(T) = C/(T - \theta) + \chi_0$, with $C = 9.850$ mol^{-1} K^{-1}, $\theta = -3.1$ K, and $\chi_0 = 0.0038$ mol^{-1}.[71] There is no significant magnetic exchange coupling between the paramagnetic Fe(II) ions because they are well-separated by the diamagnetic $[W_6S_8(CN)_6]^{6-}$ cluster anions. In fact, the effective moment *per Fe* calculated from the Curie constant[71] is $\mu_{eff} = 5.13\ \mu_B$, corresponding reasonably well to the theoretical moment of high-spin Fe(II) ($S = 2$) ion. These extended structure compounds constructed with both W_6S_8 cluster and transition metal ions are Mott insulators and not interesting in terms of electronic conduction. However, because of the appropriate orbital symmetry,[72] in contrast to the networks made of paramagnetic $[Re_6Q_8(CN)_6]^{3-}$ (Q = Se, Te) clusters,[34] there *might* be significant magnetic interactions[73,27] in this class of W_6S_8 cluster networks if the cluster is oxidized by one electron.

Summary

3-D coordination network structures can be constructed with $[W_6S_8(CN)_6]^{6-}$ cluster anions and transition metal cations M^{2+} (M = Mn, Fe, Co, Zn). They display rather different structures from the reported $[Re_6Q_8(CN)_6]^{3-/4-}$ coordination networks, probably because of the different charges of the W or Re cluster anions. These structures are rather fragile and readily lose solvent of crystallization. Magnetic studies confirm that these compounds are Mott insulators, as expected.

Acknowledgment. This work was supported by the US Department of Energy (Grant DE-FG02-87ER45298). This work made use of the Polymer Characterization Facility and the Electron & Optical Microscopy Laboratory of the Cornell Center for Materials Research (CCMR) supported by NSF under Award DMR-0079992. We thank Dr. Emil Lobkovsky for his help in X-ray crystallography and Dr. ZhengTao Xu and Prof. Stephen Lee for their helpful discussion.

Supporting Information Available: Powder X-ray diffraction pattern of sample **1** ["$(Et_4N)_5W_6S_8(CN)_6$"] as prepared, in comparison with the simulated diffraction patterns of $(Et_4N)_5W_6S_8(CN)_6$ and Curie−Weiss plots of samples **1** and **5**. A table of other unsuccessful linking reactions using $[W_6S_8(CN)_6]^{6-}$. X-ray crystallographic files (CIF) for all single-crystal structures reported. This material is available free of charge via the Internet at http://pubs.acs.org.

CM020103B

(71) The molecular weight of the sample was corrected for the loss of the crystalline water up to the point of weighing out the sample based on the data from TGA analysis (assuming water is completely gone at 500 °C).

(72) Hughbanks, T.; Hoffmann, R. *J. Am. Chem. Soc.* **1983**, *105*, 1150.

(73) Ferlay, S.; Mallah, T.; Ouahes, R.; Veillet, P.; Verdaguer, M. *Nature* **1995**, *378*, 701.